Computational Study of Noncovalent Complexes between Formamide and Formic Acid

Elsa Sánchez-García,[†] Luis A. Montero,[‡] and Wolfram Sander*[,†]

Lehrstuhl für Organische Chemie II, Ruhr-Universität Bochum, D-44780 Bochum, Germany, and Laboratorio de Química Computacional y Teórica, Facultad de Química, Universidad de la Habana, 10400, Cuba

Received: September 21, 2005; In Final Form: August 25, 2006

The geometries and binding energies of 1:1, 1:2, and 1:4 formic acid−formamide complexes (FA−FMA) are calculated by quantum chemical procedures. Vibrational spectra and intermolecular distances of the most stable FA−FMA dimers as well as the influence of the basis set superposition error (BSSE) on the geometries and energies of the dimers are also discussed. All FA−FMA dimers are optimized at the B3LYP/cc-pVTZ, the MP2/cc-pVDZ, aug-cc-pVDZ, cc-pVTZ, and aug-cc-pVTZ levels of theory to study the influence of the level of theory on the calculated geometries and energies. CCSD(T)/cc-pVTZ single-point calculations at the MP2/aug-cc-pVTZ-optimized geometries were performed as reference for estimating the quality of lower level calculations. These calculations allow us to qualitatively describe the competition between different types of hydrogen-bonding interactions in FA−FMA complexes. FA−FMA dimers are compared to other formamide complexes and to the FA−FMA crystal structure.

Introduction

For many years formic acid (FA), formamide (FMA), and their complexes with a variety of molecules have been subject to a large number of experimental and theoretical studies.[1−18] Formic acid is one of the simplest organic molecules forming hydrogen bonds in the gas, liquid, and solid state, and formamide is the simplest molecule containing a peptide linkage. Therefore, formic acid and formamide can be used as simple models of hydrogen bond interactions involving carboxylic acids and amino groups in biological systems, like protein−protein and protein−substrate interactions.[18,19]

FA−FMA complexes are very interesting hydrogen-bonded systems. In addition to their biological interest, they provide good models for studying the competition between noncovalent interactions involving nitrogen and oxygen atoms in the same molecule. As already mentioned, FA and FMA homodimers, as well as their complexes with other molecules like water and methanol, have been intensively studied.[20−23] However, only few reports are found about FA−FMA heterodimers. The computational study of the electron-density-dependent properties of FA, FMA, and their homo- and heterodimers made by Galvez et al.,[18] the crystallographic structure by Nahringbauer and Larsson in 1968,[24] and the ab initio calculations of Neuheuser et al.[8] are of special interest.

In the present work we describe several minima of the FA−FMA potential energy surface and discuss their geometries, binding energies, and vibrational spectra. The FA−FMA complexes exhibit different hydrogen-bonding interactions: NH···O, OH···O, C═O···H, C−O···H, and CH···O, making them challenging for theoretical research. The results obtained with various computational methods and basis sets are discussed, as well as the influence of the basis set superposition error (BSSE) on the calculated energies and geometries of the complexes. The 1:2 and 1:4 FA−FMA complexes are also investigated. The structures of the FA−FMA dimers and trimers are compared to those of the FMA−water and FMA−methanol dimers from literature data and with the reported FA−FMA crystal structure.

Computational Methods

The multiple minima hypersurface (MMH) approach[25−29] was used for searching configurational minima in the FA−FMA system. One thousand randomly arranged FA−FMA clusters were generated as starting points, and the resulting geometries were optimized and analyzed using PM3 and AM1[30−32] semiempirical quantum mechanical Hamiltonians. These semiempirical results provided a preliminary overview of the FA−FMA interactions, and the relevant configurations were further refined using DFT and ab initio methods. For the 1:2 and 1:4 FA−FMA complexes, 250 and 198 random geometries, respectively, were taken as starting points for the PM3 geometry optimizations.

Ab initio and DFT computations were performed using the Gaussian 98,[33] Gaussian 03,[34] and MOLPRO[35] programs. The equilibrium geometries and vibrational frequencies were calculated using second-order Møller−Plesset perturbation theory (MP2)[36] and density functional theory (DFT) with the B3LYP hybrid functional.[37,38] Pople and co-worker's 6-31G(d,p) basis set[39,40] and augmented and nonaugmented Dunning's correlation consistent double- and triple-ζ basis sets[41] (cc-pVDZ, aug-cc-pVDZ, cc-pVTZ, and aug-cc-pVTZ) were used. Single-point calculations were done with coupled clusters of single and double substitutions (with noniterative triples)[42] CCSD(T)/aug-cc-pVTZ.

The stabilization energies were calculated by subtracting the energies of the monomers from those of the complexes and corrected for the basis set superposition errors (BSSE) using the counterpoise (CP) scheme of Boys and Bernardi.[43] ZPE corrections were included.

To investigate the influence of the basis set superposition errors (BSSE) on the geometries of the complexes, the two most

* To whom correspondence should be addressed. E-mail: wolfram.sander@rub.de.
[†] Ruhr-Universität Bochum.
[‡] Universidad de la Habana.

10.1021/jp0553636 CCC: $33.50
Published on Web 11/02/2006

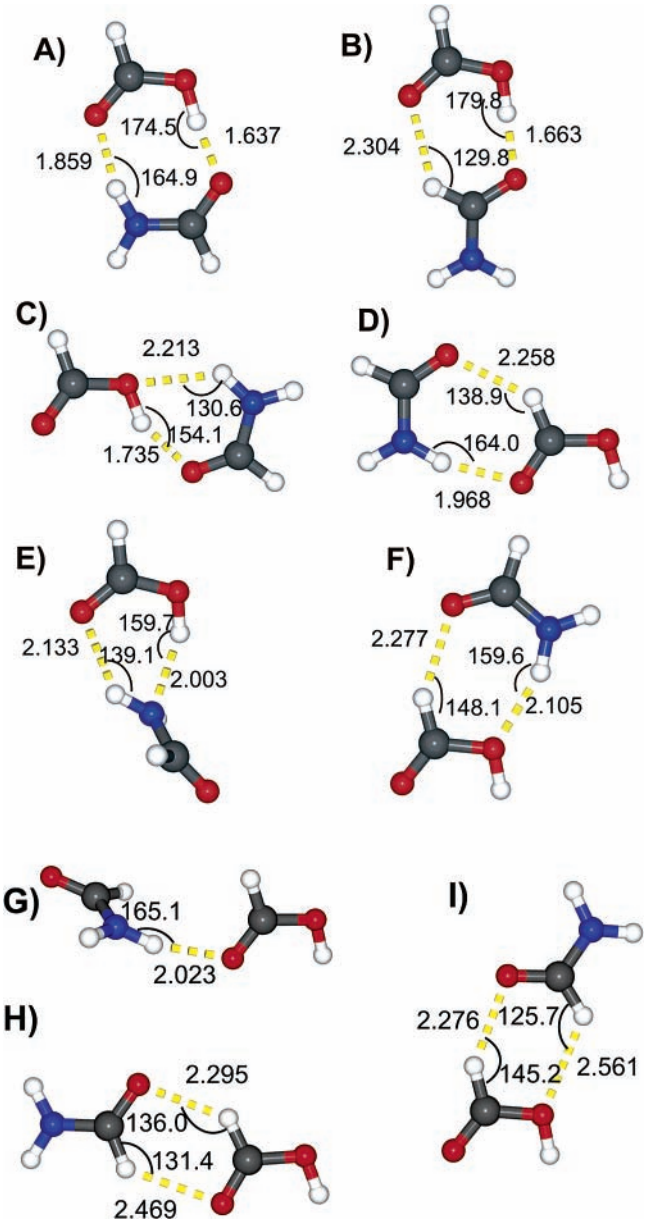

Figure 1. Calculated structures with hydrogen bond lengths (angstrom) and angles (deg) of the FA−FMA dimers A−I at the MP2/aug-cc-pVTZ level of theory.

stable dimers were optimized at the MP2/6-31G(d,p) level of theory using the CP scheme during the geometry optimization process. In addition, the geometries were optimized without BSSE at the same level of theory to compare the influence of the BSSE on the binding energies as well as on the geometries. The small 6-31G(d,p) basis set was selected for this purpose since the BSSE is more pronounced with small basis sets and, in addition, the computations are less demanding.

Results and Discussion

1. Formic Acid−Formamide Dimers. *1.1. Geometries and Binding Energies: Analysis of the Intermolecular Interactions.* Nine FA−FMA complexes A−I were localized after MMH search and refined with both DFT and MP2 calculations (Figure 1). The use of Dunning's cc-pVDZ, aug-cc-pVDZ, cc-pVTZ, and aug-cc-pVTZ basis sets (Table 1) revealed that the geometries of the complexes are almost independent of the basis sets used. Therefore, we discuss hydrogen bond distances and angles at the MP2/aug-cc-pVTZ level of theory only.

TABLE 1: Calculated Binding Energies and ZPE- and BSSE-Corrected Binding Energies (in kcal/mol) of the FA−FMA Dimers A−I[a]

	MP2						
	cc-pVDZ			aug-cc-pVDZ			cc-pVTZ
	ΔE	$\Delta E_{(ZPE)}$	$\Delta E_{(BSSE)}$	ΔE	$\Delta E_{(ZPE)}$	$\Delta E_{(BSSE)}$	ΔE
A	−18.37	−15.92	−11.60	−16.53	−14.30	−14.21	−16.90
B	−14.56	−12.57	−8.67	−12.87	−11.09	−11.03	−13.21
C	−11.38	−9.72	−6.69	−9.93	−8.36	−8.23	−10.16
D	−10.06	−8.29	−5.34	−8.97	−7.37	−7.41	−8.89
E	−10.21	−8.03	−5.19	−7.54	−5.85	−5.81	−8.04
F	−7.58	−6.33	−3.67	−6.38	−5.16	−4.97	−6.12
G	−6.57	−4.95	−3.15	−5.42	−4.34	−4.29	−5.58
H	−6.26	−5.21	−2.47	−5.50	−4.56	−4.31	−5.34
I	−5.37	−4.50	−2.15	−4.64	−3.82	−3.52	−4.37

	MP2			B3LYP		CCSD(T)/cc-pVTZ//	
	aug-cc-pVTZ			cc-pVTZ		MP2/aug-cc-pVTZ	
	ΔE	$\Delta E_{(ZPE)}$[b]	$\Delta E_{(BSSE)}$	ΔE	$\Delta E_{(ZPE)}$	ΔE	$\Delta E_{(ZPE)}$[b]
A	−16.64	−14.41	−15.25	−16.03	−13.97	−16.76	−14.53
B	−12.96	−11.18	−11.87	−12.2	−10.46	−13.21	−11.43
C	−9.95	−8.38	−8.92	−8.97	−7.53	−10.00	−8.42
D	−8.71	−7.11	−7.86	−7.77	−6.25	−9.06	−7.45
E	−7.32	−5.63	−6.37	−6.22	−4.52	−8.06	−6.37
F	−6.05	−4.83	−5.26	−4.88	−3.78	−6.24	−5.02
G	−5.2	−4.12	−4.58	−4.63	−3.59	−5.40	−4.32
H	−5.17	−4.23	−4.60	−4.37	−3.44	−5.60	−4.66
I	−4.29	−3.47	−3.73	−3.37	−2.60	−4.54	−3.71

[a] BSSE-corrected binding energies for the cc-pVDZ, aug-cc-pVDZ, and aug-cc-pVTZ basis sets at the MP2 level of theory. [b] ZPE correction from the MP2/aug-cc-pVDZ calculations.

Seven basic types of interactions (1−7) can be differentiated in the FA−FMA complexes:

(1) $NH_{FMA}\cdots O{=}C_{FA}$ interaction between the amide hydrogen atom of FMA and the carbonyl oxygen atom of FA.

(2) $C{=}O_{FMA}\cdots HO_{FA}$ interaction between the carbonyl oxygen atom of FMA and the hydroxyl hydrogen atom of FA.

(3) $(O)CH_{FMA}\cdots O{=}C_{FA}$ interaction between the aldehyde hydrogen atom of FMA and the carbonyl oxygen atom of FA.

(4) $NH_{FMA}\cdots(H)OC_{FA}$ interaction between the amide hydrogen atom of FMA and the hydroxyl oxygen atom of FA.

(5) $C{=}O_{FMA}\cdots HC(O)_{FA}$ interaction between the carbonyl oxygen atom of FMA and the aldehyde hydrogen atom of FA.

(6) $HN(H)_{FMA}\cdots HO_{FA}$ interaction between the nitrogen atom of FMA and the hydroxyl hydrogen atom of FA.

(7) $(O)CH_{FMA}\cdots(H)OC_{FA}$ interaction between the aldehyde hydrogen atom of FMA and the hydroxyl oxygen atom of FA.

The most stable FA−FMA dimer calculated is complex A with a binding energy of −14.41 kcal/mol (MP2/aug-cc-pVTZ + ZPE); the ZPE correction is taken from the MP2/aug-cc-pVDZ calculations. The energies of the other dimers B−I are also discussed at this level of theory (Table 1).

The dimer A is stabilized by interactions 1 and 2 involving both carbonyl groups and the N−H and O−H hydrogen atoms of the formamide and formic acid molecules. The binding distances are 1.859 and 1.637 Å, respectively. In dimer B (−11.18 kcal/mol) the amide hydrogen atoms of the FMA are not involved in the stabilization of the complex. Instead, the aldehyde hydrogen atom of the FMA interacts with the carbonyl oxygen atom of the FA at 2.304 Å (interaction 3). Cyclic dimer B is also stabilized by interaction 2 with a binding distance of 1.663 Å (around 0.025 Å longer than interaction 2 in complex A).

The difference between the binding energies of complexes A and B is more than 3 kcal/mol. This is explained by the different hydrogen bond capabilities of the N−H versus C−H

hydrogen atoms of FMA. Consequently, the difference between the hydrogen bond distances of interaction 1 in A and interaction 3 in B is more than 0.4 Å.

In comparison to dimer A, the FA−FMA complexes C and D are between 6 and 7 kcal/mol less stable. The binding energy of complex C is calculated to be −8.38 kcal/mol. In dimer C, as in A and B, the carbonyl oxygen atom of FMA is interacting with the hydroxyl hydrogen atom of FA (interaction 2). However, at 1.735 Å the hydrogen bond distance in C is considerably larger than in A and B (Figure 1). In dimer C the carbonyl oxygen atom of FA is not involved in the stabilization of the complex. Instead, one of the amide hydrogen atoms of FMA interacts with the hydroxyl oxygen atom of FA at a distance of 2.213 Å (interaction 4).

Dimer D has a binding energy of −7.11 kcal/mol, and it is energetically very close (about 1 kcal/mol) to dimer C. In dimer D, again both carbonyl groups of the formamide and formic acid molecules are involved in the stabilization of the complex via interaction 1 (1.968 Å hydrogen bond distance) and interaction 5 between the carbonyl oxygen atom of FMA and the aldehyde hydrogen atom of FA (hydrogen bond distance of 2.258 Å). In this case, the O−H group of the FA is not involved in the stabilization of the dimer.

The cyclic−nonplanar structure of dimer E is an interesting case. The amide group is pyramidalized and thus makes possible interaction 6 between the nitrogen atom of FMA and the O−H hydrogen atom of FA (2.003 Å). Complex E is also stabilized by the interaction 1 with a 2.133 Å distance. The calculated binding energy of dimer E is −5.63 kcal/mol.

The dimers F−I are weakly bound and energetically very close to each other. The binding energies vary between −4.83 and −3.47 kcal/mol. With the exception of the nonplanar dimer G, stabilized only by interaction 1, all dimers are cyclic. Dimer F is stabilized by interactions 4 and 5 and dimer H by interactions 3 and 5. In dimer I, interaction 5 appears together with the weakest interaction 7 between the carbonyl hydrogen atom of FMA and the hydroxyl oxygen atom of FA resulting in a large distance of 2.561 Å. In none of the F−I dimers does the hydroxyl hydrogen atom of the formic acid molecule interact with other groups.

All the complexes discussed here were produced from randomly generated geometries and not via chemical intuition. It is thus interesting to note the following:

The calculated geometries of the FA−FMA dimers A and B are in complete agreement with the calculated structures of the FA−FMA complexes proposed by Neuheuser et al.[8] and Galvez et al.[18] in their ab initio and DFT studies. Our complexes also show interesting analogies with the FMA−water and FMA−methanol dimers, which have been extensively studied. These comparisons are discussed in more detail later.

The most stable dimers A and B are those where both carbonyl groups of FMA and FA are involved in the stabilization of the complex, together with the hydroxyl hydrogen atom of FA that interacts with the carbonyl oxygen atom of FMA (interaction 2).

In the less stable complexes F−I the hydroxyl hydrogen atoms of FA are not involved in hydrogen bonds.

According to the calculated geometries and binding energies of all the FA−FMA dimers, it is possible to make some preliminary qualitative conclusions about the strength of the different interactions:

(a) $C{=}O_{FA}\cdots H{-}N_{FMA}$ (interaction 1) > $C{=}O_{FA}\cdots H{-}C_{FMA}$ (interaction 3).

(b) $C{=}O_{FMA}\cdots H{-}O_{FA}$ (interaction 2) > $C{=}O_{FMA}\cdots H{-}C_{FA}$ (interaction 5).

(c) $NH_{FMA}\cdots O{=}C_{FA}$(interaction 1) > $NH_{FMA}\cdots(H)OC_{FA}$ (interaction 4).

(d) $OH_{FA}\cdots O{=}C_{FMA}$(interaction 2) > $OH_{FA}\cdots NH_{FMA}$ (interaction 6).

(e) $CH_{FMA}\cdots O{=}C_{FA}$(interaction 3) > $CH_{FMA}\cdots(H)OC_{FA}$-(interaction 7).

(f) The CH group in the formic acid molecule only interacts with the O=C group of the formamide molecule (interaction 5).

This allows us to qualitatively compare the hydrogen bond acceptors and donors in the FA−FMA dimers.

(a) Donors: $OH > NH > CH_{FMA} > CH_{FA}$

(b) Acceptors: $C{=}O_{FMA} > C{=}O_{FA}$. The order of the proton donor ability of the hydrogen atoms linked to C, N, and O heteroatoms corresponds to the increase of the electronegativity from carbon to oxygen. To compare the hydrogen bond acceptor capability of the carbonyl group of FMA with that of the carbonyl group of FA is more complicated. In this case, the order is based on the relative binding energies and distances in the complexes.

It is interesting to mention that for the FMA−water and FMA−methanol dimers the binding energy to the carbonyl group of FMA is slightly more favorable than to the amide group.[21,22,44] In the most stable FA−FMA dimer A both interactions are present, and the distance between the carbonyl oxygen atom of FMA and the hydroxyl hydrogen atom of FA is nearly 0.2 Å shorter than the hydrogen bond distance between the amide hydrogen atom of FMA and the carbonyl oxygen atom of FA (Figure 1).

In agreement with Neuheuser et al.'s observations,[8] the weakest C−H···O interaction still contributes significantly to the interaction energy in the FA−FMA system, for example in dimer B.

1.2. Comparison with Other Dimers. The presence of carbonyl groups in both FMA and FA results in additional stabilizations which do not exist in the water−formamide (W−FMA) and the methanol−formamide (M−FMA) complexes. Nevertheless, there are very interesting analogies among all the FMA complexes with water, methanol, and formic acid.[21,22,44] (Figure 2).

Three stable W−FMA structures were described by Fu et al.[21] using DFT and MP2 methods with large basis sets. In all cases the main interaction is $OH_w\cdots O{=}C_{FMA}$. FW I and FW II are the two more stable W−FMA calculated complexes. They are cyclic dimers with additional $NH_{FMA}\cdots O{-}H_W$ and $CH_{FMA}\cdots O{-}H_W$ interactions, respectively (Figure 2). Their geometries have some similarities with the structures of some of the FA−FMA dimers.

In the FA−FMA dimer A the carbonyl group of the formamide molecule interacts with the hydroxyl hydrogen atom of the formic acid resembling the interaction between the carbonyl group of the formamide and the hydroxyl hydrogen atom of water in the FW I complex. The amide hydrogen atom of FMA interacts with the carbonyl oxygen atom of FA in a similar way as the $NH_{FMA}\cdots O{-}H_W$ interaction in the FW I formamide−water complex.

The water−formamide dimer FW II shows the $C{=}O_{FMA}\cdots HO_w$ interaction (similar to the $C{=}O_{FMA}\cdots HO_{FA}$ in complexes A and B) and the $CH_{FMA}\cdots O{-}H_W$ (similar to the $CH_{FMA}\cdots O{=}C_{FA}$ interaction in complex B).

Four stable formamide−methanol (M−FMA) dimers have been studied by Fu et al. using DFT and ab initio methods with

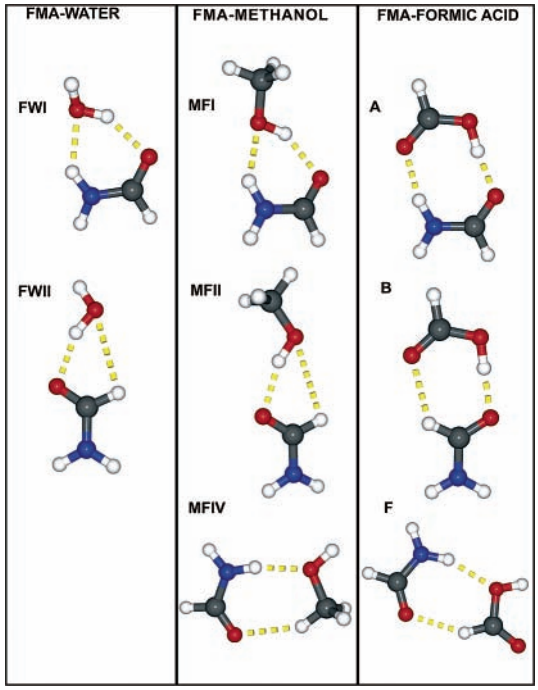

Figure 2. B3LYP structures of FMA−water, FMA−methanol, and selected FMA−FA dimers.

various basis sets.[22] The two most stable M−FMA complexes have similar geometries compared to those of the FA−FMA and W−FMA dimers.

MF I is a cyclic dimer with $OH_M\cdots O{=}C_{FMA}$ and $NH_{FMA}\cdots O{-}H_M$ interactions. The MF II dimer shows the $OH_M\cdots O{=}C_{FMA}$ and $CH_{FMA}\cdots O{-}H_M$ interactions. Both structures are similar to the A and B FA−FMA dimers.

MF IV compares very well with the FA−FMA dimer F. They are both cyclic dimers stabilized by the $NH_{FMA}\cdots(H)OC_{FA(MET)}$ interaction between the amide hydrogen atom of FMA and the hydroxyl oxygen atom of the FA or methanol molecules. The second interaction is the $C{=}O_{FMA}\cdots HC_{FA}$ in the case of complex F. The MF IV dimer shows the $C{=}O_{FMA}\cdots HC_M$ interaction between the carbonyl oxygen atom of FMA and one hydrogen atom from the methyl group of the methanol molecule.

Formamide−formic acid dimers have been studied before using ab initio and DFT methods. Neuheuser et al. calculated five noncyclic and ring H-bonded FA−FMA structures as a model for the interactions in supramolecular complexes of dicarboxylic acids and dimethylformamide.[8] Pacios performed ab initio calculations of the most stable FMA−FA dimer A.[45] Galvez et al. studied the variation of electron's density properties with the intermolecular distance for various cyclic dimers, including the most stable FA−FMA complex.[18] Neuheuser et al.'s, Pacios, and Galvez et al.'s studies corroborate our FA−FMA dimers A and B as the most stable calculated geometries in the formic acid−formamide system. This agreement confirms the reliability of the MMH procedure for localizing the minima in noncovalent complexes.

1.3. Methods and Basis Set Influence on the Calculated Geometries and Binding Energies of the FMA−FA Dimers. Table 2 lists some selected intra- and intermolecular distances and hydrogen bond angles at various levels of theory for selected FA−FMA dimers. Complex A is discussed because it is the most stable calculated FA−FMA dimer. The weaker complex D has been selected due to its very weak $C{=}O_{FMA}\cdots H{-}C_{FA}$ interaction. In addition, intermolecular distances for complex B are presented.

TABLE 2: Comparison of Selected Intramolecular and Intermolecular Parameters in the FA−FMA Dimers A, B, and D at the Different Levels of Theory[a]

	B3LYP	MP2			
	cc-pVTZ	cc-pVDZ	aug-cc-pVDZ	cc-pVTZ	aug-cc-pVTZ
		Monomer			
$O{-}H_{FA}$	0.970	0.975	0.975	0.970	0.971
$C{-}H_{FA}$	1.097	1.108	1.103	1.092	1.092
$N{-}H_{FMA}$[b]	1.006	1.014	1.012	1.004	1.006
$C{=}O_{FA}$	1.197	1.209	1.215	1.203	1.205
$C{=}O_{FMA}$	1.209	1.220	1.228	1.215	1.218
		Dimer A			
$O{-}H_{FA}$	1.006	1.005	1.006	1.004	1.005
$N{-}H_{FMA}$[b]	1.022	1.027	1.027	1.019	1.020
$C{=}O_{FA}$	1.214	1.225	1.231	1.219	1.221
$C{=}O_{FMA}$	1.229	1.237	1.245	1.232	1.235
$NH_{FMA}\cdots O{=}C_{FA}$	1.879	1.872	1.871	1.853	1.859
$C{=}O_{FMA}\cdots HO_{FA}$	1.643	1.661	1.657	1.634	1.637
$< NH_{FMA}\cdots O_{FA}$	164.77	164.65	165.35	165.48	164.90
$< OH_{FA}\cdots O_{FMA}$	175.70	173.95	173.98	173.82	174.51
		Dimer D			
$C{-}H_{FA}$	1.095	1.104	1.101	1.091	1.092
$N{-}H_{FMA}$[b]	1.016	1.022	1.021	1.014	1.015
$C{=}O_{FA}$	1.207	1.219	1.225	1.213	1.214
$C{=}O_{FMA}$	1.218	1.227	1.236	1.222	1.225
$NH_{FMA}\cdots O{=}C_{FA}$	2.006	1.992	1.981	1.968	1.968
$C{=}O_{FMA}\cdots HC(O)_{FA}$	2.295	2.258	2.267	2.251	2.257
$< NH_{FMA}\cdots O_{FA}$	163.31	164.40	164.52	164.64	163.99
$< CH_{FA}\cdots O_{FMA}$	138.65	140.70	139.51	140.57	138.88
		Dimer B			
$O{-}H_{FA}$	1.001	1.001	1.002	0.998	1.000
$C{=}O_{FA}$	1.209	1.220	1.226	1.214	1.216
$C{=}O_{FMA}$	1.225	1.235	1.242	1.229	1.231
$C{=}O_{FMA}\cdots HO_{FA}$	1.676	1.683	1.682	1.663	1.663
$(O)CH_{FMA}\cdots O{=}C_{FA}$	2.350	2.308	2.317	2.303	2.304

[a] Distances are in angstrom and angles in deg. [b] Amide hydrogen atom in the cis position relative to the carbonyl oxygen atom of the formamide.

The $O{-}H_{FA}$ bond lengths in dimer A are not sensitive to the method or the basis set used for the calculations (Table 2). However, the $N{-}H_{FMA}$ intramolecular distances of the interacting amide hydrogen atoms vary in both complexes A and D substantially with the basis set. At the MP2 level of theory, the calculated $N{-}H_{FMA}$ bond lengths with the cc-pVDZ basis set are 0.007 Å larger than with the cc-pVTZ basis, whereas inclusion of diffuse functions has only a minor influence. The B3LYP/cc-pVTZ-calculated bond lengths are only 0.002−0.003 Å larger than the MP2/cc-pVTZ values.

The $C{-}H_{FA}$ bond lengths in complex D behave in a similar way. In this case the difference between the MP2 double- and triple-ζ basis set is even more pronounced (0.0103−0.009 Å). The MP2/cc-pVTZ and aug-cc-pVTZ $C{-}H_{FA}$ distances are basically the same and very similar to the B3LYP/cc-pVTZ ones. The MP2/cc-pVDZ $C{-}H_{FA}$ bond length is 0.003 Å larger than the MP2/aug-cc-pVDZ-calculated value. The C=O carbonyl bond lengths of the FMA and FA molecules in dimers A and D show a little more dependence on the basis sets. At the MP2 level of theory the C=O distances increase with the addition of diffuse functions (aug) in the double- and triple-ζ basis sets. This variation is less pronounced with the triple-ζ basis set. The B3LYP/cc-pVTZ carbonyl bond lengths are of 0.006−0.003 Å shorter than the MP2/cc-pVTZ values.

The $NH_{FMA}\cdots O{=}C_{FA}$ distances in both A and D dimers are 0.026 and 0.038 Å, respectively, larger at the B3LYP level of theory compared to those of the MP2 calculations with the same basis sets. In the MP2 calculations the $NH_{FMA}\cdots O{=}C_{FA}$ binding distances decrease from the double- to the triple-ζ basis sets.

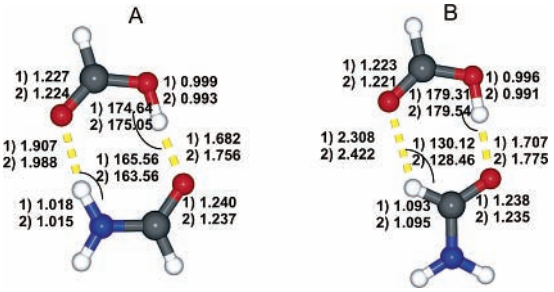

Figure 3. MP2/6-31G(d,p) geometries with inter- and intramolecular lengths (angstrom) and hydrogen bond angles (deg) of dimers A and B: (1) optimized without BSSE corrections; (2) optimized with BSSE corrections.

The behavior of the $C{=}O_{FMA}\cdots HO_{FA}$ (dimer A) and the $C{=}O_{FMA}\cdots H{-}C_{FA}$ (dimer D) distances is very similar, in general. The calculated hydrogen bond angles are comparable in all cases. Intermolecular distances in complex B are basically not dependent on the augmentation of the basis sets.

The B3LYP calculations show a tendency to give a little larger value for the intermolecular binding distances, compared to the MP2 values with the same basis set. However, there is no considerable difference between the B3LYP- and the MP2-calculated geometries for the FA−FMA dimers. Reliable geometries for the weak interacting FA−FMA dimers are also calculated using the B3LYP density functional. At the MP2 level of theory, we found basically no change of the geometries when the basis set is augmented by adding diffuse functions.

In the FA−FMA dimers, the MP2/cc-pVDZ calculations have a tendency to overestimate the binding energies (Table 1). The double-ζ energies compare better to the CCSD(T)/cc-pVTZ calculations when the augmented functions are added. At the MP2 level, using triple-ζ basis sets augmented and nonaugmented, the results are very similar to those of the CCSD(T)/cc-pVTZ single-point calculations. The B3LYP/cc-pVTZ binding energies are smaller than the MP2 and CCSD(T) energies.

We also confirm that at the MP2 level of theory the cc-pVTZ basis set provides a very adequate description of our system; it is in general not necessary to use the expensive aug-cc-pVTZ basis set, according with what we have found in previous work with weakly interacting complexes.[27−29]

1.4. Effect of the BSSE on the Calculated Geometries and Binding Energies. BSSE corrections have been calculated for all FA−FMA dimers at the MP2 level of theory with the cc-pVDZ, aug-cc-pVDZ, and aug-cc-pVTZ basis sets. As expected, the BSSE decreases with increasing size of the basis sets. That can be noticed by comparing the ΔE (binding energies without corrections) with $\Delta E_{(BSSE)}$ (BSSE-corrected binding energies) in Table 1. For example, in complex A with MP2/cc-pVDZ the BSSE correction is 6.77 kcal/mol, compared to only 2.32 and 1.39 kcal/mol at the MP2/aug-cc-pVDZ and MP2/aug-cc-pVTZ levels of theory, respectively.

In addition, FA−FMA dimers A and B were optimized at the MP2/6-31G(d,p) level of theory using the counterpoise (CP) scheme to evaluate the influence of BSSE on the calculated energies and geometries.

The intramolecular bond distances in the FA and FMA molecules are almost not effected by the inclusion of BSSE corrections during the optimization processes (Figure 3). In all cases the difference between the bond distances was in the order of 10^{-3} Å or less. Only the intermolecular distances $C{=}O_{FA}\cdots H{-}N_{FMA}$ (interaction 1), $C{=}O_{FMA}\cdots H{-}O_{FA}$ (interaction 2), and $C{=}O_{FA}\cdots H{-}C_{FMA}$ (interaction 3) are significantly influenced by BSSE. Especially for the weaker interaction 3 the BSSE-optimized distance $C{=}O_{FA}\cdots H{-}C_{FMA}$ is almost 0.12 Å larger than the non-BSSE-optimized distance. Hydrogen bond angles are less sensitive to BSSE corrections (Figure 3). Thus, the geometrical changes introduced by BSSE corrections are very limited, and the basic geometries and interactions in FA−FMA complexes do not depend on the inclusion of BSSE during the optimization process, in accordance with our previous observations.[29]

TABLE 3: Comparison of the Binding Energies of the Calculated FA−FMA Dimers A and B at the MP2/6-31G(d,p) Level of Theory Including (or Not) BSSE Corrections in the Optimization Processes

	MP2/6-31G(d,p)			
	optimization with BSSE		optimization without BSSE	
	ΔE	$\Delta E_{(BSSE)}$	ΔE	$\Delta E_{(BSSE)}$
dimer A	−18.03	−13.39	−18.22	−13.19
dimer B	−14.88	−10.23	−14.31	−10.08

TABLE 4: Comparison between the Experimental (Ar Matrix, 10 K) and the Calculated B3LYP Vibrational Frequencies (in cm^{-1}) of Formic Acid and Formamide Monomers, Shift, and Factor of Correction

experimental	computed frequencies B3LYP/cc-pVTZ	shift and factor of correction (exp/B3LYP freq)[a]	mode of assignment
3549.9	3722.1	172.2 (0.954)	ν_{OH}[b]
3066.0	3043.8	−22.2 (1.007)	ν_{CH}[b]
1766.9	1826.2	59.3 (0.967)	$\nu_{C=O}$[b]
1103.5	1125.0	21.5 (0.981)	ν_{CO}[b]
1739.1	1803.8	64.7 (0.964)	$\nu_{C=O}$[c]
2882.9	2931.0	48.9 (0.984)	ν_{CH}[c]
3547.4	3718.2	170.8 (0.954)	ν_{asNH2}[c]
3426.6	3579.9	153.3 (0.957)	ν_{sNH2}[c]

[a] Shifts are calculated as the difference between the computed and the experimental frequencies. [b] Formic acid fundamental modes. [c] Formamide fundamental modes.

It is therefore not surprising that the binding energies of dimers A and B are almost independent of BSSE corrections during geometry optimization. For complexes A and B the calculated BSSE corrections are 4−5 kcal/mol, and the differences in binding energies between the BSSE-optimized and the non-BSSE-optimized geometries are in the range of 0.19−0.57 kcal/mol only (Table 3).

1.5. Intramolecular Distances and Vibrational Frequencies: Calculated Spectra and Rotational Constants. The vibrational frequencies of all the FA−FMA dimers have been calculated at the B3LYP/cc-pVTZ, MP2/cc-pVDZ, and MP2/aug-cc-pVDZ levels of theory. We discuss here the B3LYP/cc-pVTZ vibrational frequencies and selected intermolecular distances for complexes A and B. On the basis of experimental and B3LYP/cc-pVTZ-calculated vibrational frequencies of the monomers, the frequency shifts and correction factors for some molecular vibrations of complexes A and B are estimated (Table 4) to accurately match calculated with experimental frequencies (Table 5).

In comparison to the monomers, intramolecular distances and the corresponding vibrational frequencies in the complexes are perturbed as a consequence of the intermolecular interactions (Tables 2 and 5). In complexes A and B the O−H stretching vibrations of the FA molecule show the largest red shifts with −677 and −585 cm^{-1}, respectively (Tables 2 and 5). This demonstrates the strong interaction between the OH hydrogen atom of FA and the carbonyl oxygen atom of FMA (Figure 1) resulting in an elongation of the OH bonds of 0.036 and 0.031 Å, respectively, for complexes A and B (B3LYP/cc-pVTZ, Table 2).

TABLE 5: Calculated B3LYP/cc-pVTZ Vibrational Frequencies (in cm^{-1}) of Dimers A and B and Frequency Shift in the Complex, from the Isolated Monomer (in Parentheses) (Predicted Frequencies after Scaling)

monomer	dimer A		dimer B		
B3LYP/cc-pVTZ	calculated	predicted[a]	calculated	predicted[a]	assignment
	2983.7				
	3012.4				
3722.1	3044.8 (*−677.3*)	2904.7	3136.7 (*−585.4*)	2992.4	ν_{OH}[b,c]
1826.2	1779.8 (*−46.4*)	1721.1	1788.5 (*−37.7*)	1729.5	$\nu_{C=O}$[b]
1125.0	1256.5 (*+131.5*)	1232.6	1230.6 (*+105.6*)	1207.2	ν_{CO}[b]
1803.8	1729.9 (*−73.9*)	1667.6	1732.3 (*−71.5*)	1669.9	$\nu_{C=O}$[d]
3718.2	3675.5 (*−42.7*)	3506.4	3715.8 (*−2.4*)	3544.9	ν_{asNH2}[d]
3579.9	3348.5 (*−231.4*)	3204.5	3579.4 (*−0.5*)	3425.5	ν_{sNH2}[d]

[a] Predicted frequencies after scaling the individual frequencies with a scaling factor obtained by comparing calculated vs experimental frequencies of the corresponding monomer bands (Table 4). [b] Formic acid. [c] In the case of complex A, there is a very strong coupling between the ν_{OH} and the ν_{CH} vibrations of formic acid and formamide. The same happens for the $\nu_{C=O}$ vibrations of formic acid and formamide. [d] Formamide.

The carbonyl stretching frequencies of the FA molecules in dimers A and B are calculated to be shifted by −46 and −38 cm^{-1}. The C═O_{FA} bond lengths in A and B increase by 0.017 and 0.012 Å compared to those of the monomers. The red shift for dimer B is 8 cm^{-1} less than for dimer A. This difference is caused by the stronger C═O_{FA}···H−N_{FMA} interaction (interaction 1) in dimer A compared to the weaker C═O_{FA}···H−C_{FMA} interaction (interaction 3) in dimer B.

The carbonyl stretching frequency shifts of the FMA molecules are −74 and −71 cm^{-1}. The C═O_{FMA} bond lengths in the dimers A and B increases by 0.020 and 0.016 Å, respectively. According to the structure of the complex, only in dimer A is a significant shift (−231 and −43 cm^{-1}) for the symmetrical and antisymmetrical vibrations of the N−H group, respectively, predicted. The intramolecular N−H bond distance of the interacting NH group of FMA in complex A is consequently 0.016 Å larger than in the FMA monomer.

2. Larger Systems. The weak interactions between FMA and FA create a very flat intermolecular energy surface. That makes the analysis of systems larger than dimers even more complicated. It would take huge computational efforts to get a complete description of the possible geometries for trimers and larger aggregates. However, there are very interesting correlations between the geometries of the FA−FMA dimers and the calculated structures of larger systems.

2.1. 1:2 Formic Acid−Formamide Complexes. Figure 4 shows a selection of the most stable calculated 1:2 FA−FMA complexes T−A to T−G and their B3LYP/cc-pVTZ binding energies with and without ZPE corrections. Trimer T−H is much less stable compared to T−A, but is included in our selection in order to compare with the crystal structure. It is important to remark, once again, that all the trimer structures are found starting from a large amount of randomly generated geometries calculated with semiempirical Hamiltonians and later refined at the B3LYP/cc-pVTZ level of theory.

T−A is the most stable calculated trimer with a binding energy of −22.22 kcal/mol. T−B is energetically very close to T−A with −21.94 kcal/mol (Figure 4). It is interesting to compare the T−A and T−B geometries with the structure of the dimers. The part of trimer T−A where the FA and FMA molecules interact with each other is similar to the FA−FMA dimer B (Figure 1). But due to the presence of a second interacting formamide molecule, the intermolecular C═O_{FA}··· H−C_{FMA} and C═O_{FMA}···H−O_{FA} distances are 0.031 and 0.008 Å larger, respectively, compared to those of dimer B at the same level of theory (Table 2, Figure 4). The FMA−FMA interactions in trimer T−A reproduce the structure of the most stable formamide homodimer.

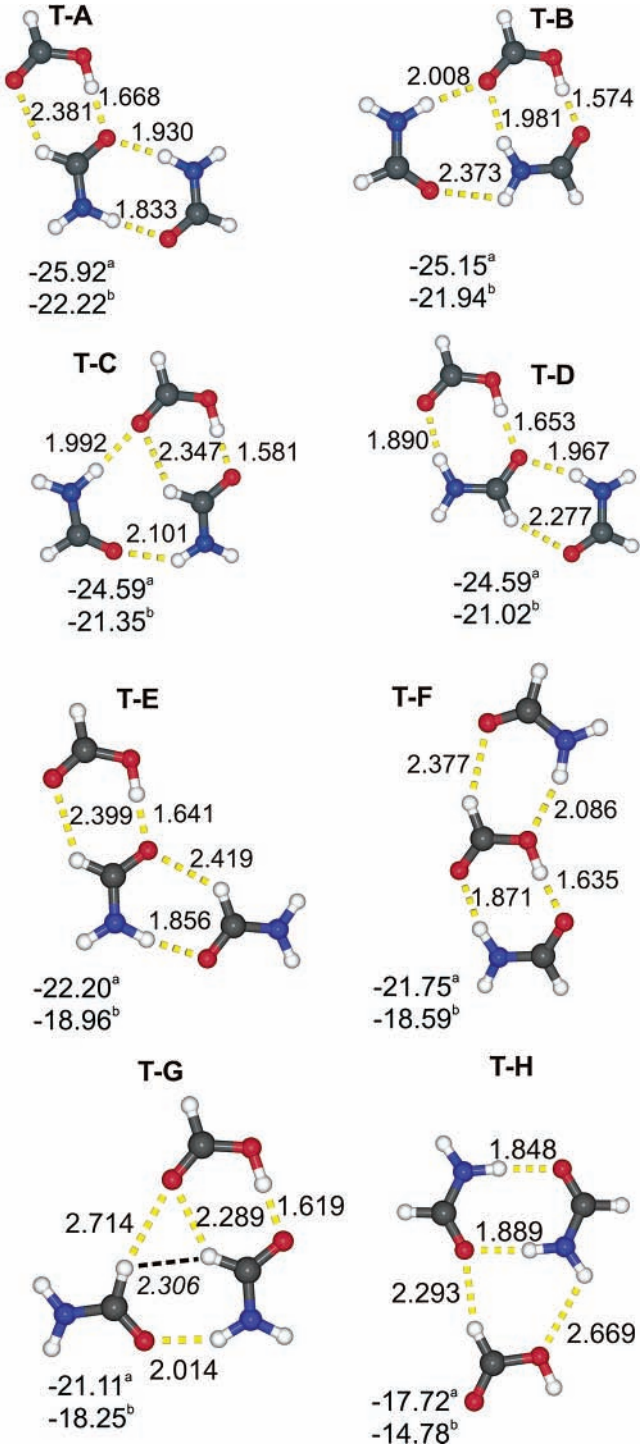

Figure 4. Calculated structures with hydrogen bond lengths (angstrom) of the 1:2 FA−FMA complexes T−A to T−G at the B3LYP/cc-pVTZ level of theory: a = B3LYP/cc-pVTZ binding energies; b = B3LYP/cc-pVTZ binding energies, ZPE-corrected (kcal/mol).

In trimer T−B, the FA interactions with FMA disturb the structure of the FA−FMA dimer A. The carbonyl oxygen atom of FA shows an additional interaction with one amide hydrogen atom of the second FMA molecule. This causes an elongation of 0.102 Å of the C═O_{FA}···H−N_{FMA} distance compared to that

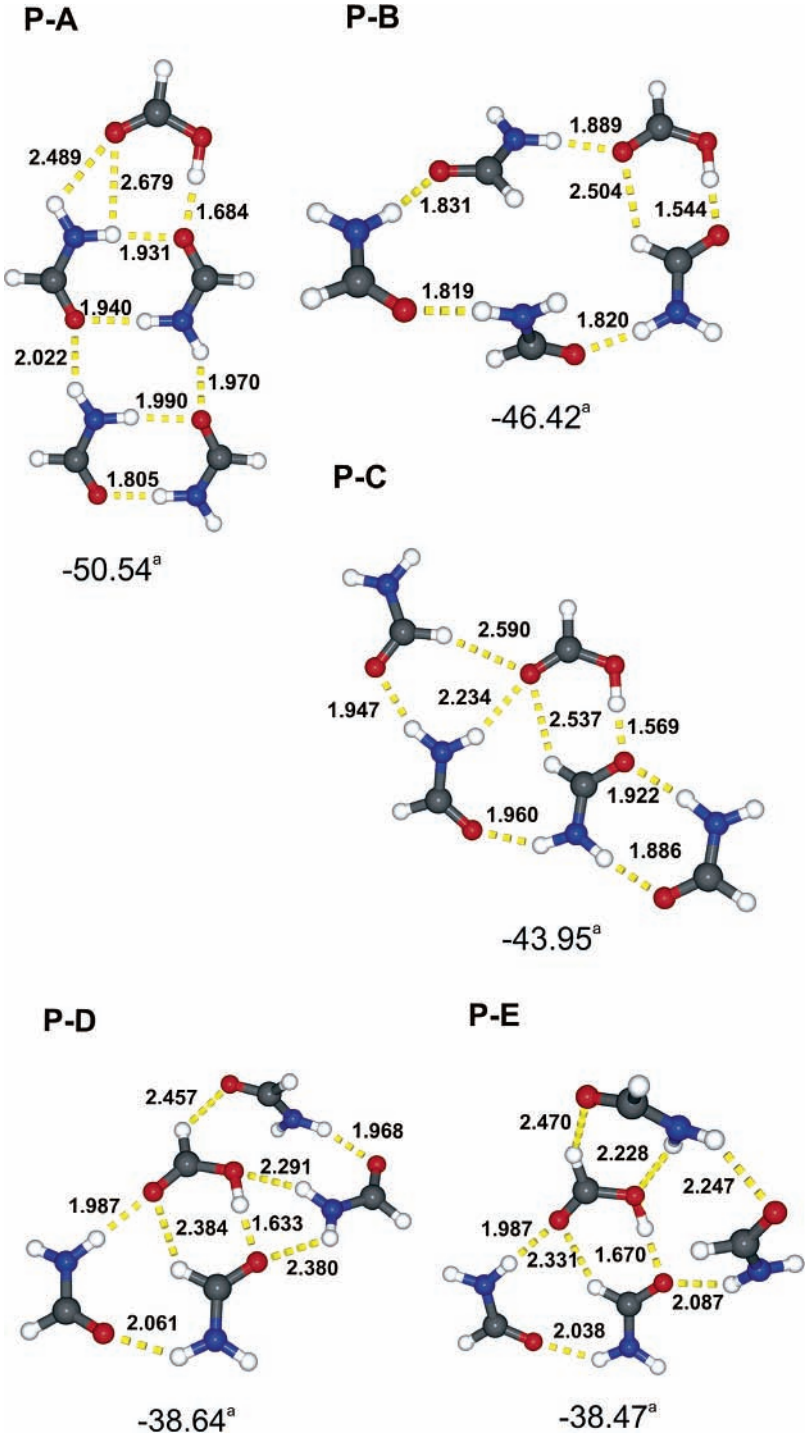

Figure 5. Calculated structures with hydrogen bond lengths (angstrom) of the 1:4 FA−FMA complexes P−A to P−E at the B3LYP/cc-pVTZ level of theory: a = B3LYP/cc-pVTZ binding energies (kcal/mol).

of dimer A. The $C{=}O_{FMA}\cdots H{-}O_{FA}$ distance in trimer T−B is also 0.069 Å larger in comparison to that of dimer A. (Table 2, Figure 4).

The trimers T−C and T−D are very close energetically to each other with binding energies of −21.35 and −21.02 kcal/mol, respectively. Again, the main interactions between FA and FMA in T−C resemble the FA−FMA dimer B, but the intermolecular distances are shorter compared to those of the dimer (Figure 4, Table 2). In this case, one amide hydrogen atom of the second FMA molecule shows an additional interaction with the carbonyl oxygen atom of the FA molecule.

T−E, T−F, and T−G have calculated binding energies of −18.96, −18.59, and −18.25 kcal/mol, respectively. But in the case of complex T−G there is one imaginary out-of-plane vibration at −15 cm^{-1} that is related with the repulsive interaction at 2.306 Å between the two aldehyde hydrogen atoms of FMA molecules (Figure 4). The geometry of the T−G complex at the B3LYP/6-31++G (d,p) level of theory is very similar, but there is no imaginary vibration, and the distance between the two aldehyde hydrogen atoms of the FMA molecules is 2.314 Å.

It is interesting to notice that in the trimers T−A, T−C, T−E, and T−G the interactions between the FA and one FMA molecule reproduce the geometry of the FA−FMA dimer B. In the same way, interactions in trimers T−B, T−D, and T−F resemble the structure of dimer A. Complex T−F is the only

with no direct interactions between the two FMA molecules. Instead, the interactions between FA and the second molecule of FMA resemble the structure of the FA−FMA dimer F (Figure 1). In the T−A, T−D, and T−E trimers the FA molecule interacts with only one molecule of FMA, and the system is additionally stabilized by the FMA−FMA attractions.

The T−H complex is less stable, since the carbonyl group and the hydroxyl hydrogen atom of the FA molecule are not directly interacting with the FMA molecules. The stabilizing FA−FMA interactions in T−H are the same as in the FA−FMA dimer F, the $C{=}O_{FMA}\cdots H{-}C_{FA}$ (interaction 5) and the $NH_{FMA}\cdots(H)OC_{FA}$ (interaction 4); however, in this case the FA interacts with two molecules of FMA. These two molecules of FMA form the structure of the cyclic most stable FMA homodimer.

2.2. 1:4 FA−FMA Complexes. The 1:4 FA−FMA complexes have been calculated starting from 198 arbitrary geometries that were optimized at the semiempirical level. A selection of complexes was refined at the B3LYP/cc-pVTZ level of theory. (Figure 5).

P−A is the most stable of the calculated pentamers with a binding energy of −50.54 kcal/mol. Complexes P−B and P−C are energetically close with binding energies of −46.42 and −43.95 kcal/mol, respectively. The binding energies of P−D and P−E are very similar, −38.64 and −38.47 kcal/mol.

The structure of the P−A complex is very interesting. The two pairs of FMA molecules form two FMA cyclic homodimers, which then interact with each other. The FA molecule stabilizes the complex with the same type of interaction that appears in the FA−FMA dimer A (Figure 1). The difference is that in P−A the FA molecule interacts with the two closest FMA molecules, and the FA carbonyl oxygen atom cooperates with two amide hydrogen atoms. In all the other complexes (P−B to P−E) the FA molecule interacts with one FMA molecule (FMA-a) with the $C{=}O_{FMA}\cdots H{-}O_{FA}$ and $C{=}O_{FA}\cdots H{-}C_{FMA}$ interactions, forming the FA−FMA dimer B (Figure 1).

By comparison with the 1:2 FA−FMA complexes it is easy to identify the structure of the T−C trimer as part of the P−C, P−D, and P−E complexes. The P−C pentamer is even more interesting, since it combines the geometries of both the T−A and T−C trimers (Figure 4). Considering the FA molecule, the FMA-a, and the FMA molecule at the right side of FMA-a, we get the geometry of trimer T−A. Consequently, if we look at the interactions between FA, FMA-a, and the FMA molecule at the left side of FMA-a, there is trimer T−C.

3. Comparison of FMA−FA Complexes with the Crystal Structure. The complexity of the FA−FMA crystal structure cannot be entirely described by a small number of FA−FMA complexes. However, interesting structural similarities can be noticed. Three sections of the FA−FMA crystal structure are presented in Figure 6, whereas Figure 7 shows a large fragment of the FA−FMA crystal structure.[24]

The same type of interactions (1−4) that have been discussed above for the FA−FMA dimers are present in the crystal structure. The geometry of dimer B is clearly reproduced in the FA−FMA crystal interactions of fragments FA and FMA2 (Figures 1 and 6). In both cases the carbonyl group of the FA interacts preferentially out-of-plane with another molecule.

The geometry of the trimer T−A is also very similar to the marked selection in the FMA2 section (Figure 4), and trimer T−H describes the geometry of the interactions between the FA molecule and the two FMA molecules forming the FMA cyclic homodimer in section FA (Figure 6).

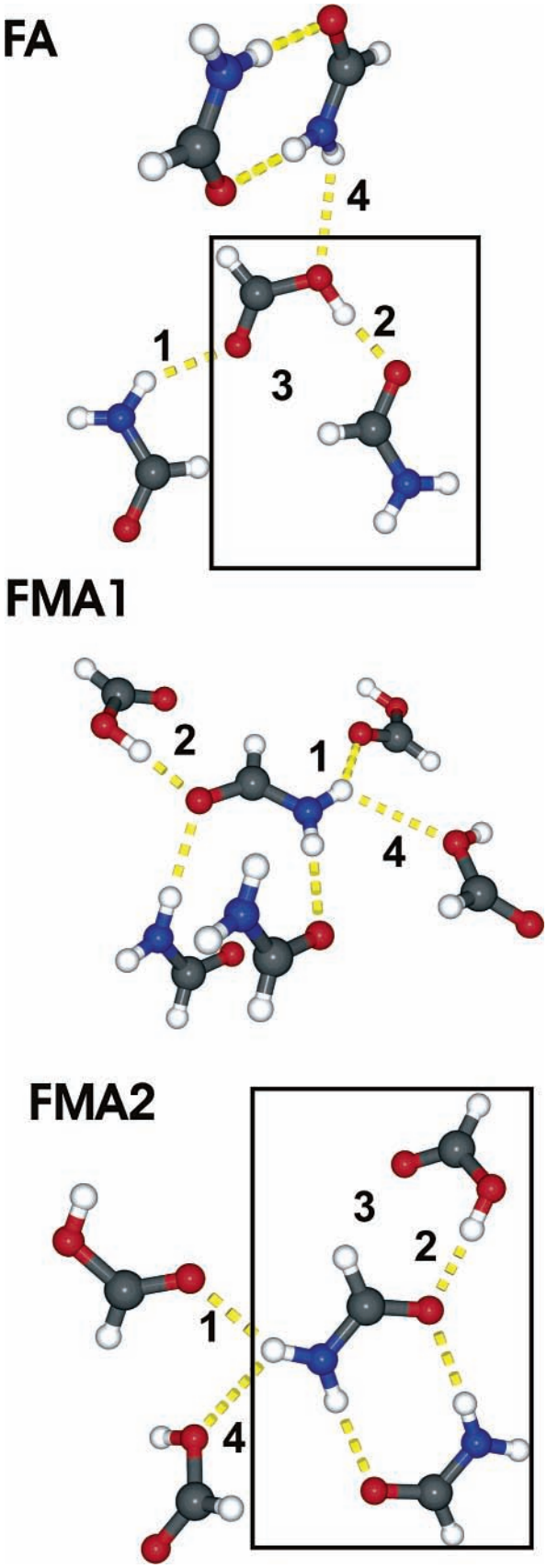

Figure 6. Selected sections of the FMA−FA crystal structure (ref 24).

Conclusion

The geometries of the FA−FMA dimers are calculated starting from randomly generated molecular arrangements using the MMH procedure. The structures of the FA−FMA dimers

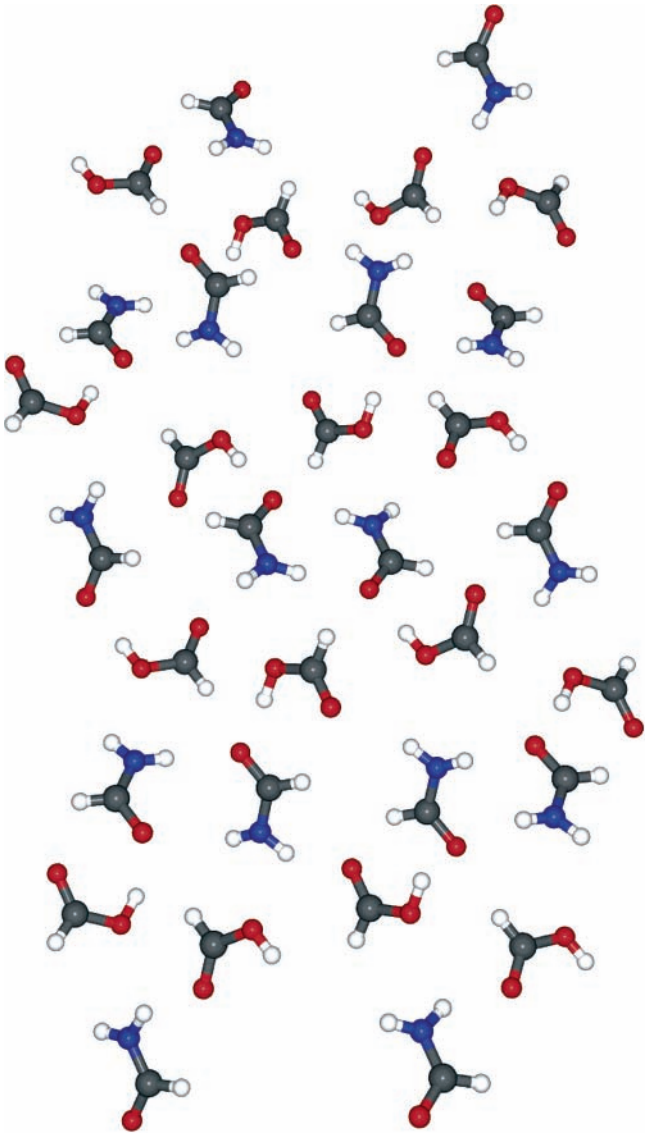

Figure 7. FMA−FA crystal structure (ref 24).

A and B are in excellent agreement with the geometries of the FA−FMA dimers reported in the literature. Our complexes also show interesting analogies with the FMA−water and FMA−methanol dimers. This confirms the quality of the MMH procedure as a very useful tool for reliably localizing minima in noncovalent complexes without referring to previous knowledge of the structure of supramolecular complexes or to "chemical intuition". The calculated geometries and binding energies of the FA−FMA dimers allows us to discuss the various competitive individual molecular interactions in the complexes.

The B3LYP density functional with the cc-pVTZ basis set provides reliable geometries for the FA−FMA complexes. At the MP2 level of theory, we found basically no change of the geometries when the basis set is augmented by adding diffuse functions. At the MP2 level cc-pVDZ calculations show a tendency to overestimate the binding energies; however, triple-ζ basis sets either augmented or nonaugmented result in binding energies very similar to those from CCSD(T)/cc-pVTZ single-point calculations. A noticeable point is that the geometries and energies of the FA−FMA dimers A and B do not change considerably with the inclusion of BSSE corrections during the optimization process.

The distortion of the intramolecular distances and vibrational frequencies in the FA−FMA dimers A and B compared to those of the monomers are discussed, and reliable vibrational frequencies are predicted. The empirically corrected frequencies should allow for the experimental detection of these complexes in matrix isolation or gas-phase studies.

The calculated geometries and binding energies of 1:2 and 1:4 FA−FMA complexes show very interesting similarities with the FA−FMA dimers and with the FA−FMA crystal structure. Of special interest are structural motifs found in the crystal structure that are already present in complexes of very few molecules. This could lead to an in-depth knowledge of the complex processes of molecular nucleation and crystal growth.

Acknowledgment. This work was financially supported by the Deutsche Forschungsgemeinschaft (Forschergruppe 618) and the Fonds der Chemischen Industrie. We thank Dr. Holger Bettinger for helpful discussions.

References and Notes

(1) Agranat, I.; Riggs, N. V.; Radom, L. *J. Chem. Soc., Chem. Commun.* **1991**, 80−81.
(2) Borisenko, K. B.; Bock, C. W.; Hargittai, I. *THEOCHEM* **1995**, *332*, 161−169.
(3) Chocholousova, J.; Vacek, J.; Hobza, P. *Phys. Chem. Chem. Phys.* **2002**, *4*, 2119−2122.
(4) Del Bene, J. E.; Kochenour, W. L. *J. Am. Chem. Soc.* **1976**, *98*, 2041−2046.
(5) Chang, Y. T.; Yamaguchi, Y.; Miller, W. H.; Schaefer, H. F., III. *J. Am. Chem. Soc.* **1987**, *109*, 7245−7253.
(6) Hayashi, S.; Umemura, J.; Kato, S.; Morokuma, K. *J. Phys. Chem.* **1984**, *88*, 1330−1334.
(7) Hobza, P.; Havlas, Z. *Theor. Chem. Acc.* **1998**, *99*, 372−377.
(8) Neuheuser, T.; Hess, B. A.; Reutel, C.; Weber, E. *J. Phys. Chem.* **1994**, *98*, 6459−6467.
(9) Turi, L. *J. Phys. Chem.* **1996**, *100*, 11285−11291.
(10) Qian, W.; Krimm, S. *J. Phys. Chem. A* **2002**, *106*, 11663−11671.
(11) Gantenberg, M.; Halupka, M.; Sander, W. *Chem.−Eur. J.* **2000**, *6*, 1865−1869.
(12) Florian, J.; Johnson, B. G. *J. Phys. Chem.* **1995**, *99*, 5899−5908.
(13) Bende, A.; Vibok, A.; Halasz, G. J.; Suhai, S. *Int. J. Quantum Chem.* **2001**, *84*, 617−622.
(14) Cabaleiro-Lago, E. M.; Rios, M. A. *J. Chem. Phys.* **1999**, *110*, 6782−6791.
(15) Lu, J.-f.; Zhou, Z.-y.; Wu, Q.-y.; Zhao, G. *THEOCHEM* **2005**, *724*, 107−114.
(16) Podolyan, Y.; Gorb, L.; Leszczynski, J. *J. Phys. Chem. A* **2002**, *106*, 12103−12109.
(17) Sponer, J.; Hobza, P. *J. Phys. Chem. A* **2000**, *104*, 4592−4597.
(18) Galvez, O.; Gomez, P. C.; Pacios, L. F. *J. Chem. Phys.* **2003**, *118*, 4878−4895.
(19) Rozas, I.; Alkorta, I.; Elguero, J. *J. Phys. Chem. B* **2004**, *108*, 3335−3341.
(20) Zhou, Z.; Shi, Y.; Zhou, X. *J. Phys. Chem. A* **2004**, *108*, 813−822.
(21) Fu, A.; Du, D.; Zhou, Z. *THEOCHEM* **2003**, *623*, 315−325.
(22) Fu, A.; Du, D.; Zhou, Z. *Int. J. Quantum Chem.* **2004**, *97*, 865−875.
(23) Coitino, E. L.; Irving, K.; Rama, J.; Iglesias, A.; Paulino, M.; Ventura, O. N. *THEOCHEM* **1990**, *69*, 405−426.
(24) Nahringbauer, I.; Larsson, G. *Ark. Kemi* **1968**, *30*, 91−102.
(25) Montero, L. A.; Esteva, A. M.; Molina, J.; Zapardiel, A.; Hernandez, L.; Marquez, H.; Acosta, A. *J. Am. Chem. Soc.* **1998**, *120*, 12023−12033.
(26) Montero, L. A.; Molina, J.; Fabian, J. *Int. J. Quantum Chem.* **2000**, *79*, 8−16.
(27) George, L.; Sanchez-Garcia, E.; Sander, W. *J. Phys. Chem. A* **2003**, *107*, 6850−6858.
(28) Sanchez-Garcia, E.; George, L.; Montero, L. A.; Sander, W. *J. Phys. Chem. A* **2004**, *108*, 11846−11854.
(29) Sanchez-Garcia, E.; Studentkowski, M.; Montero, L. A.; Sander, W. *ChemPhysChem* **2005**, *6*, 618−624.
(30) Dewar, M. J. S.; Zoebisch, E. G.; Healy, E. F.; Stewart, J. J. P. *J. Am. Chem. Soc.* **1985**, *107*, 3902−3909.
(31) Stewart, J. J. P. *MOPAC*, version 6.0, Universidad de La Habana, 1993−1997.
(32) Stewart, J. J. P. *J. Comput. Chem.* **1989**, *10*, 209−264.

(33) Frisch, M. J.; Trucks, G. W.; Schlegel, H. B.; Scuseria, G. E.; Robb, M. A.; Cheeseman, J. R.; Zakrzewski, V. G.; Montgomery, J. A., Jr.; Stratmann, R. E.; Burant, J. C.; Dapprich, S.; Millam, J. M.; Daniels, A. D.; Kudin, K. N.; Strain, M. C.; Farkas, O.; Tomasi, J.; Barone, V.; Cossi, M.; Cammi, R.; Mennucci, B.; Pomelli, C.; Adamo, C.; Clifford, S.; Ochterski, J.; Petersson, G. A.; Ayala, P. Y.; Cui, Q.; Morokuma, K.; Malick, D. K.; Rabuck, A. D.; Raghavachari, K.; Foresman, J. B.; Cioslowski, J.; Ortiz, J. V.; Stefanov, B. B.; Liu, G.; Liashenko, A.; Piskorz, P.; Komaromi, I.; Martin, R. L.; Fox, D. J.; Keith, T.; Al-Laham, M. A.; Peng, C. Y.; Nanayakkara, A.; Gonzalez, C.; Challacombe, M.; Gill, P. M. W.; Johnson, B. G.; Chen, W.; Wong, M. W.; Andres, J. L.; Head-Gordon, M.; Replogle, E. S.; Pople, J. A. *Gaussian 98*, revision A.11.1; Gaussian, Inc.: Pittsburgh, PA, 1998.

(34) Frisch, M. J.; Trucks, G. W.; Schlegel, H. B.; Scuseria, G. E.; Robb, M. A.; Cheeseman, J. R.; Montgomery, J. A., Jr.; Vreven, T.; Kudin, K. N.; Burant, J. C.; Millam, J. M.; Iyengar, S. S.; Tomasi, J.; Barone, V.; Mennucci, B.; Cossi, M.; Scalmani, G.; Rega, N.; Petersson, G. A.; Nakatsuji, H.; Hada, M.; Ehara, M.; Toyota, K.; Fukuda, R.; Hasegawa, J.; Ishida, M.; Nakajima, T.; Honda, Y.; Kitao, O.; Nakai, H.; Klene, M.; Li, X.; Knox, J. E.; Hratchian, H. P.; Cross, J. B.; Bakken, V.; Adamo, C.; Jaramillo, J.; Gomperts, R.; Stratmann, R. E.; Yazyev, O.; Austin, A. J.; Cammi, R.; Pomelli, C.; Ochterski, J. W.; Ayala, P. Y.; Morokuma, K.; Voth, G. A.; Salvador, P.; Dannenberg, J. J.; Zakrzewski, V. G.; Dapprich, S.; Daniels, A. D.; Strain, M. C.; Farkas, O.; Malick, D. K.; Rabuck, A. D.; Raghavachari, K.; Foresman, J. B.; Ortiz, J. V.; Cui, Q.; Baboul, A. G.; Clifford, S.; Cioslowski, J.; Stefanov, B. B.; Liu, G.; Liashenko, A.; Piskorz, P.; Komaromi, I.; Martin, R. L.; Fox, D. J.; Keith, T.; Al-Laham, M. A.; Peng, C. Y.; Nanayakkara, A.; Challacombe, M.; Gill, P. M. W.; Johnson, B.; Chen, W.; Wong, M. W.; Gonzalez, C.; Pople, J. A.; *Gaussian 03*, revision B.04; Gaussian, Inc.: Pittsburgh, PA, 2003.

(35) Werner, H.-J.; Knowles, P.J.; Schütz, M.; Lindh, R.; Celani, P.; Korona, T.; Rauhut, G.; Manby, F. R.; Amos, R. D.; Bernhardsson, A.; Berning, A.; Cooper, D. L.; Deegan, M. J. O.; Dobbyn, A. J.; Eckert, F.; Hampel, C. ; Hertzer, G.; Lloyd, A. W.; McNicholas, S. J.; Meyer, W.; Mura, M. E.; Nicklass, A.; Palmieri, P.; Pitzer, R.; Schumann, U.; Stoll, H.; Stone, A. J.; Tarroni, R.; Thorsteinsson, T. *MOLPRO*; version 2000.1, Universität Stuttgart: Stuttgart, Germany.

(36) Moller, C.; Plesset, M. S. *Phys. Rev.* **1934**, *46*, 618−622.

(37) Becke, A. D. *J. Chem. Phys.* **1993**, *98*, 5648−5652.

(38) Lee, C.; Yang, W.; Parr, R. G. *Phys. Rev. B: Condens. Matter Mater. Phys.* **1988**, *37*, 785−789.

(39) Krishnan, R.; Binkley, J. S.; Seeger, R.; Pople, J. A. *J. Chem. Phys.* **1980**, *72*, 650−654.

(40) Frisch, M. J.; Pople, J. A.; Binkley, J. S. *J. Chem. Phys.* **1984**, *80*, 3265−3269.

(41) Dunning, T. H., Jr. *J. Chem. Phys.* **1989**, *90*, 1007−1023.

(42) Raghavachari, K.; Trucks, G. W.; Pople, J. A.; Head-Gordon, M. *Chem. Phys. Lett.* **1989**, *157*, 479−483.

(43) Boys, S. F.; Bernardi, F. *Mol. Phys.* **1970**, *19*, 553.

(44) Jansien, P. G.; Stevens, W. J. *J. Chem. Phys.* **1986**, *84*, 3271−3277.

(45) Pacios, L. F. *J. Phys. Chem. A* **2004**, *108*, 1177−1188.